Chapter 10 – MISSION ANALYSIS AND SIMULATION

10.1 GENERAL

This chapter is dedicated to the simulation tools developed during the PILASTER program, especially in the areas of eye-safety and system performance analysis. The theoretical and empirical models described in the previous chapters were used in the software programs, allowing a complete definition of test/ training laser mission constraints and operational feasibility, together with post-mission data analysis. The assumptions adopted for implementation of the various mathematical algorithms in the PC simulation/ analysis programs are presented in this chapter, together with results of some relevant simulation runs performed.

10.2 EYE-SAFETY VERIFICATION PROGRAMS

A discussion about the key-parameters considered for laser safety analysis was presented in Chapter 6, together with description of the relevant geometric elements of typical ALS/GLS operational tasks, and an underline of the safety verification algorithms developed for the various cases. In this paragraph, we detail the various assumptions adopted for implementing two MATLAB™ Eye-safety Verification Programs (EVP) for both ALS (A-EVP) and GLS (G-EVP) systems. Furthermore, the results of simulations are presented, relative to the ELOP PLD ground LTD and to a typical airborne LTD system (the Thompson CLDP technical characteristics are not presented due to military classification), for operation at the PILASTER test range.

10.2.1 A-EVP and G-EVP Simulation Assumptions

The following assumptions were adopted for implementation of the A-EVP and G-EVP programs:

- **The reflecting surface (BZ) is perfectly planar**: This assumption is conservative in the case of convex surfaces laying within the BZ (these would in fact determine an increase of divergence with consequent reduction of the energy density at the observer location); while, in the case of concave surfaces, it is extremely improbable that their presence in the BZ can determine focusing (reduction of divergence) of the laser beam.
- **The laser beam reflection is totally specular**: This assumption is conservative from a safety point of view, because the energy density of a specularly reflected laser beam is always greater than in the real case. This is because reflection from any practical surface is always characterised by the co-hesitance of two components: a diffuse component and a specular component, each more or less important depending on the physical characteristics of the reflecting surface.
- **For the A-SVP the entire A-BZ is considered as a specular reflector**: This is a conservative assumption for eye-safety calculations. Moreover, considering the entire BZ as the actual reflector, the presence of any reflecting material inside the BZ is not relevant for safety (i.e., objects removal is not required within the BZ, but only evacuation of the ground personnel).
- **For the G-SVP the target surface is considered as a diffuse reflector**: This is a condition that was imposed when designing the PILASTER targets.
- **Atmospheric attenuation of the laser beam is not considered**: This assumption implies that the entire energy emitted by the LTD reaches the observer location. This is obviously a conservative assumption, since atmospheric absorption and scattering effects are neglected.
- **The NOHD is calculated for direct vision of a Gaussian laser beam**: The assumption of direct vision is conservative, since the observer is assumed to look directly at the laser source, instead of

a reflected beam; while a Gaussian distribution of the laser beam is applicable in practice for most ALS systems (e.g., Thompson CLDP).

- **Allowance is made for atmospheric scintillation effects**: This assumption is conservative as it implies, in the absence of C_n measurements, that $OHD_S = 2.662 \cdot NOHD$.
- **For the A-SVP a significant instability of the system LOS is considered**: Both in the TRACK and in the SLAVE modes of operation of the A-LTD, the point of intersection of the LOS with the ground is not fixed. Based on data relative to various real A-LTD systems, the maximum instability was assumed to be 20 m in SLAVE mode and 4 m in TRACK mode.

Moreover, it is considered that **no magnifying instruments are used** in the test range (i.e., the NOHD can be used instead of the EOHD). This is not properly an assumption, since a prohibition can be imposed by the range authorities (as long as cinetheodolites are not required; in which event proper filtering measures are essential).

10.2.2 A-EVP Airborne LTD Simulation

The probabilities of hazardous events during real missions, for a typical airborne laser target designator (A-LTD) are presented in Table 10-1 (see also Table 6-1 and Table 6-2 in Chapter 6). For completeness of information, a description of the missions listed in the table, is give below:

- **Ferry Flight**, is a transfer mission in which the WSO does not use any of the LTD operating modes and the WSO control panel is in the SAFE position;
- **DRY Attack**, is a simulated attack mission (without activation of the laser FIRE mode), carried out with the WSO control panel in the SAFE position; and
- **HOT Attack**, is a real attack mission (with or without actual bomb dropping), in which all operational modes of the LTD are used.

Table 10-1: The Probabilities of Hazardous Events during Real Missions

MISSION	*Operative Conditions*	*LTD Modes*	*Hazard Probability*
Ferry Flight	N.A.	LTD ON/ Laser FIRE	$P_{SAFE \to FIRE}$= 7E-6
DRY Attack (in the range)	Controlled range target, visually acquired	LTD ON/ TRACK-SLAVE/ Laser SAFE	P_{ROT}*$P_{SAFE \to FIRE}$= 1.4E-9
HOT Attack (in the range)	Controlled range target, visually acquired	LTD ON/ TRACK-SLAVE/ Laser FIRE	P_{ROT}=2E-6
DRY Attack (outside range)	Target visually acquired	LTD ON/ Laser SAFE	$P_{SAFE \to FIRE}$=7E-4
HOT Attack (outside range)	NOT POSSIBLE IN ANY CONDITION		

As indicated in Table 10-1, during HOT/DRY attacks carried out in the test range, it is essential that the target (either hard or soft) is visually acquired by the WSO and it is desirable that the clearance for firing the laser is obtained by a Laser Safety Officer, monitoring at a ground control station (connected with the aircraft trough an encrypted video telemetry system) the correct pointing of the system LOS.

Using the data in Table 10-2, relative to the main technical characteristics of a generic airborne laser target designator (A-LTD) system (technical data relative to the CLDP are not presented due to military classification), together with data already presented in Table 6-1, Table 6-2 and Table 10-1 (relative to the same generic A-LTD), we give an example of a practical application of the EVP simulation program described in the previous paragraphs.

Table 10-2: A-LTD Design Characteristics

Wavelength	1064 nm
Beam Diameter	60 mm
Beam Divergence	0.2 mrad
Output Energy	100 mJ
Pulse Duration	10^{-9} sec
Pulse Repetition Rate	13 Hz
Max LOS Misalignment	SLAVE mode: 40 m TRACK mode: 4 m

The MPE_P (i.e., MPE for a single pulse) is 0.05 J/m^2. Therefore, with the previously stated assumptions, the NOHD equates to 7679 m (i.e., about 25200 ft), and the OHD_S to 20426 m. This means that, in the absence of scintillation effects (i.e., low turbulence), the HA does not exist as long as the aircraft is flying at an altitude higher than 25200 ft (in case of turbulence, the required aircraft altitude exceeds the maximum altitude of any existing military aircraft!).

In order to carry out missions at lower altitudes, the hazard probabilities given in Table 10-1, have to be accepted. For instance, if the maximum acceptable risk level is associated with a probability of hazardous event of 1E-5, all missions can be carried out, with exception for DRY/HOT attacks outside the test range. If, however, the probability level is set to 1E-8, none of the missions is possible, with the exception of DRY attacks inside the test range.

Simulation results relative to the aircraft flight limitations during laser firing (i.e., minimum and maximum distance of the aircraft from the target) applicable to the PILASTER range with a maximum evacuation area of 4.3 km radius around the target location (A-EBZ), are shown in Figure 10-1 and Figure 10-2. The tolerance of the aircraft height is ±100 ft. The ground-speed lower limit is 250 kts. No restrictions to the aircraft trajectory are applied in the horizontal plane.

Figure 10-1: A-LTD TRACK Mode Simulation Results.

Figure 10-2: A-LTD SLAVE Mode Simulation Results.

10.2.3 G-EVP ELOP-PLD Simulation Results

The ELOP-PLD Ground LTD (G-LTD) system technical characteristics relevant to eye-safety are listed in Table 10-3.

Table 10-3: ELOP-PLD Technical Characteristics

Parameter	Value
Wavelength	*1064 nm*
Output Energy	*130 mJ*
Beam Divergence	*130 μrad (80% of the output energy)*
Pulse Duration	*19 nsec*
Beam Output Diameter	*90 mm*
Maximum laser/LOS Misalignment	*80 μrad*
Laser PRF	*10 or 20 Hz*

Since the divergence was specified at 80% of total output energy, the *1/e* divergence required for safety calculations was obtained using the following equation:

$$\Phi_{1/e} = \Phi_{\eta}\sqrt{\frac{ln(1-0.632)}{ln(1-\eta)}} \tag{10.1}$$

where Φ_{η} is the given divergence (Φ_{η} = 0.13 mrad) and η is the relative percentage of total energy (i.e., $\eta = 0.8$). For the ELOP-PLD, we obtained $\Phi_{1/e}$ = 0.102 mrad. The NOHD and OHDS calculated for PRF = 10 Hz (used for LGB) and for various times of exposure (T_E), are shown in Figure 10-3.

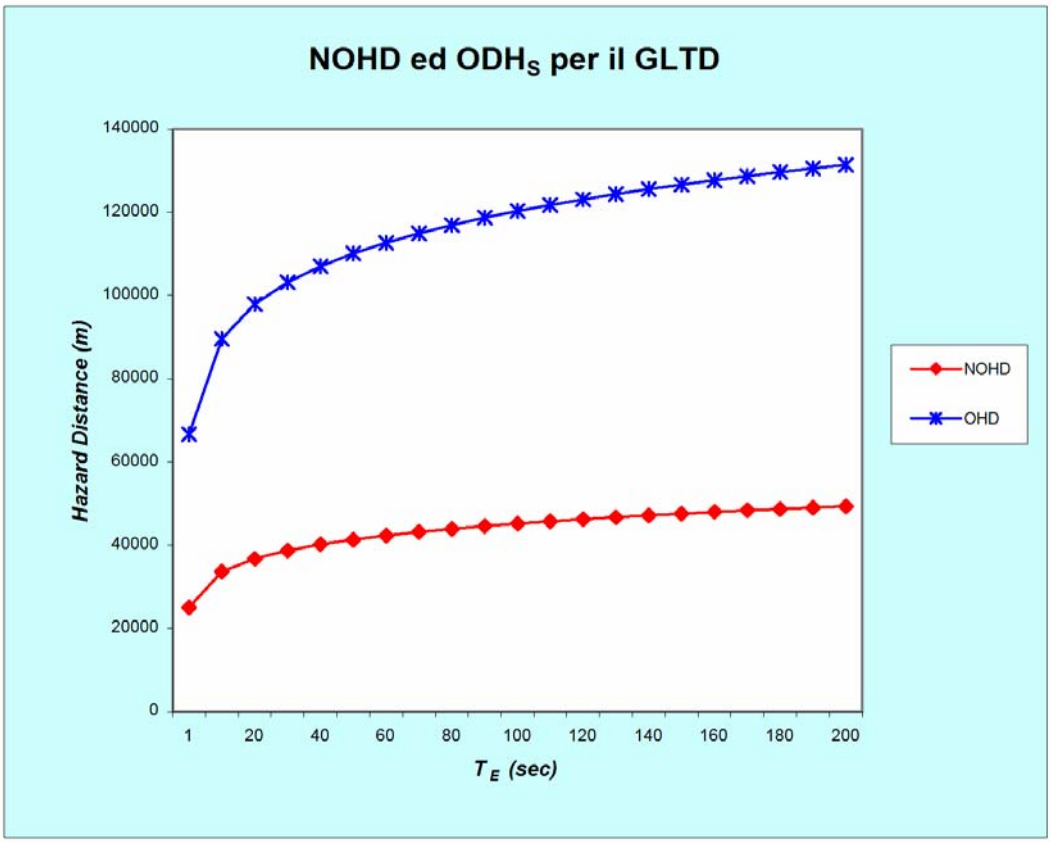

Figure 10-3: ELOP-PLD Ocular Hazard Distances.

Taking into account the experimental results obtained during the ground experimental activities performed with the ELOP-PLD, together with temporary scintillation phenomena in the presence of high turbulence (i.e., $C_n \geq 2.43 \cdot 10^{-7}$), remarkable and very frequent spreading effects where observed, especially for long LTD-to-target slant-ranges. In order to account for this in the ELOP-PLD eye safety calculations, the BZE described in Chapter 6 (and not the NOHD) was calculated considering the maximum measured laser spot divergence (calculated from spot diameter measurements) geometric divergence of the ELOP-PLD systems (Φ_{eff} = 0.25 mrad) instead of the *1/e* divergence ($\Phi_{1/e}$ = 0.102 mrad).

Figure 10-4 shows the curves relative to the maximum LTD-target slant-ranges admitted (with various horizontal incidence angles), calculated in accordance with the G-LTD safety verification Procedure N° 1 described in Chapter 6, considering various target surface dimensions. Particularly, the PILASTER permanent and modular targets dimensions have been considered (i.e., 10 × 10 m and 9.76 × 7.925 m respectively), together with the PILASTER modular target square sections (i.e., dimensions of 7.32 × 7.32 m, 4.88 × 4.88 m and 2.44 × 2.44 m).

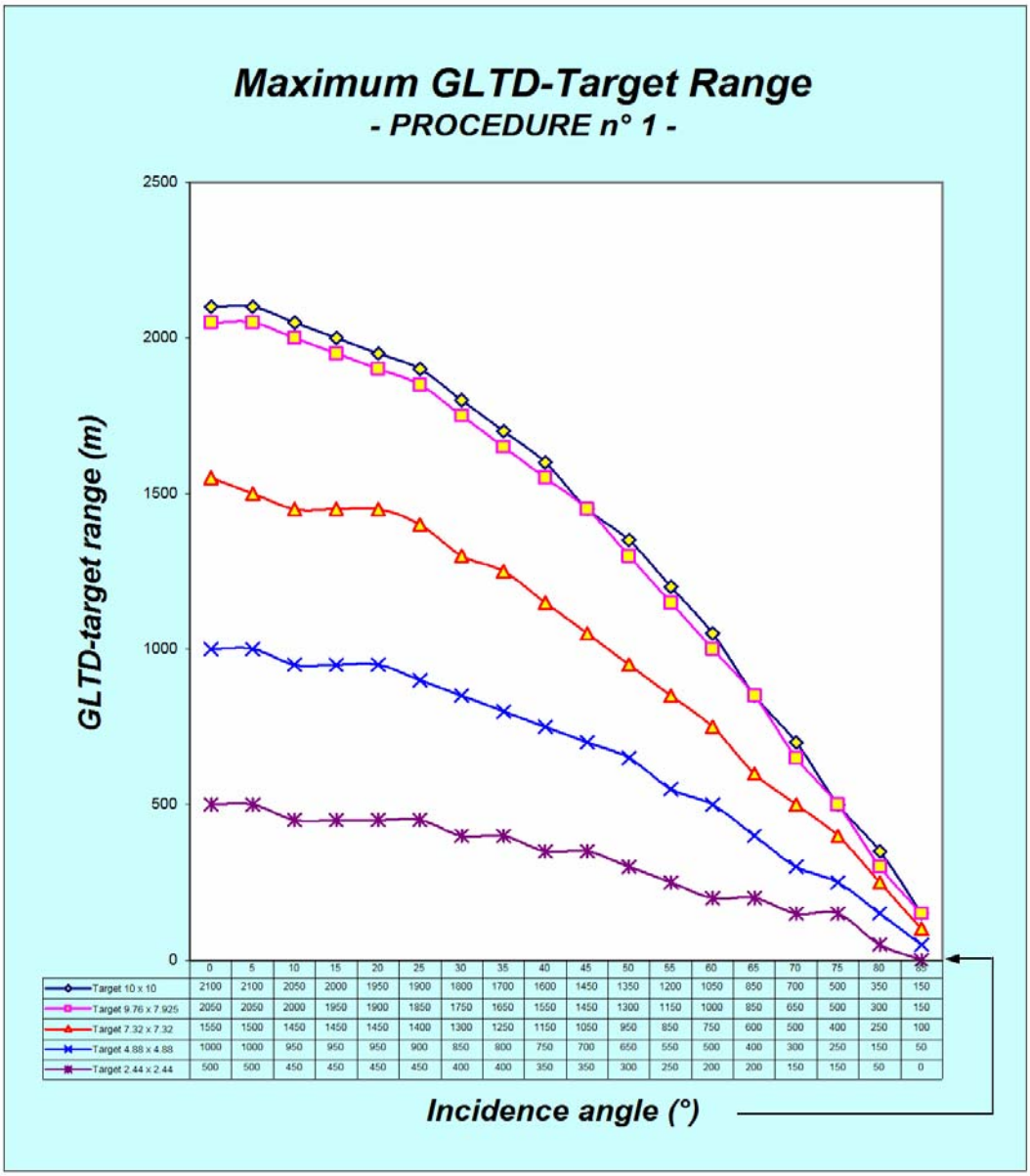

	0	5	10	15	20	25	30	35	40	45	50	55	60	65	70	75	80	85
Target 10 x 10	2100	2100	2050	2000	1950	1900	1800	1700	1600	1450	1350	1200	1050	850	700	500	350	150
Target 9.76 x 7.925	2050	2050	2000	1950	1900	1850	1750	1650	1550	1450	1300	1150	1000	850	650	500	300	150
Target 7.32 x 7.32	1550	1500	1450	1450	1450	1400	1300	1250	1150	1050	950	850	750	600	500	400	250	100
Target 4.88 x 4.88	1000	1000	950	950	950	900	850	800	750	700	650	550	500	400	300	250	150	50
Target 2.44 x 2.44	500	500	450	450	450	450	400	400	350	350	300	250	200	200	150	150	50	0

Figure 10-4: Maximum ELOP-PLD Range vs. Incidence Angle (Procedure N° 1).

Figure 10-5 shows the curves relative to the maximum LTD-target slant-ranges admitted (vs. incidence angle), calculated in accordance with the G-LTD safety verification Procedure N° 4 described in Chapter 6 (i.e., PILASTER NIR-camera real-time monitoring), considering the various PILASTER targets dimensions.

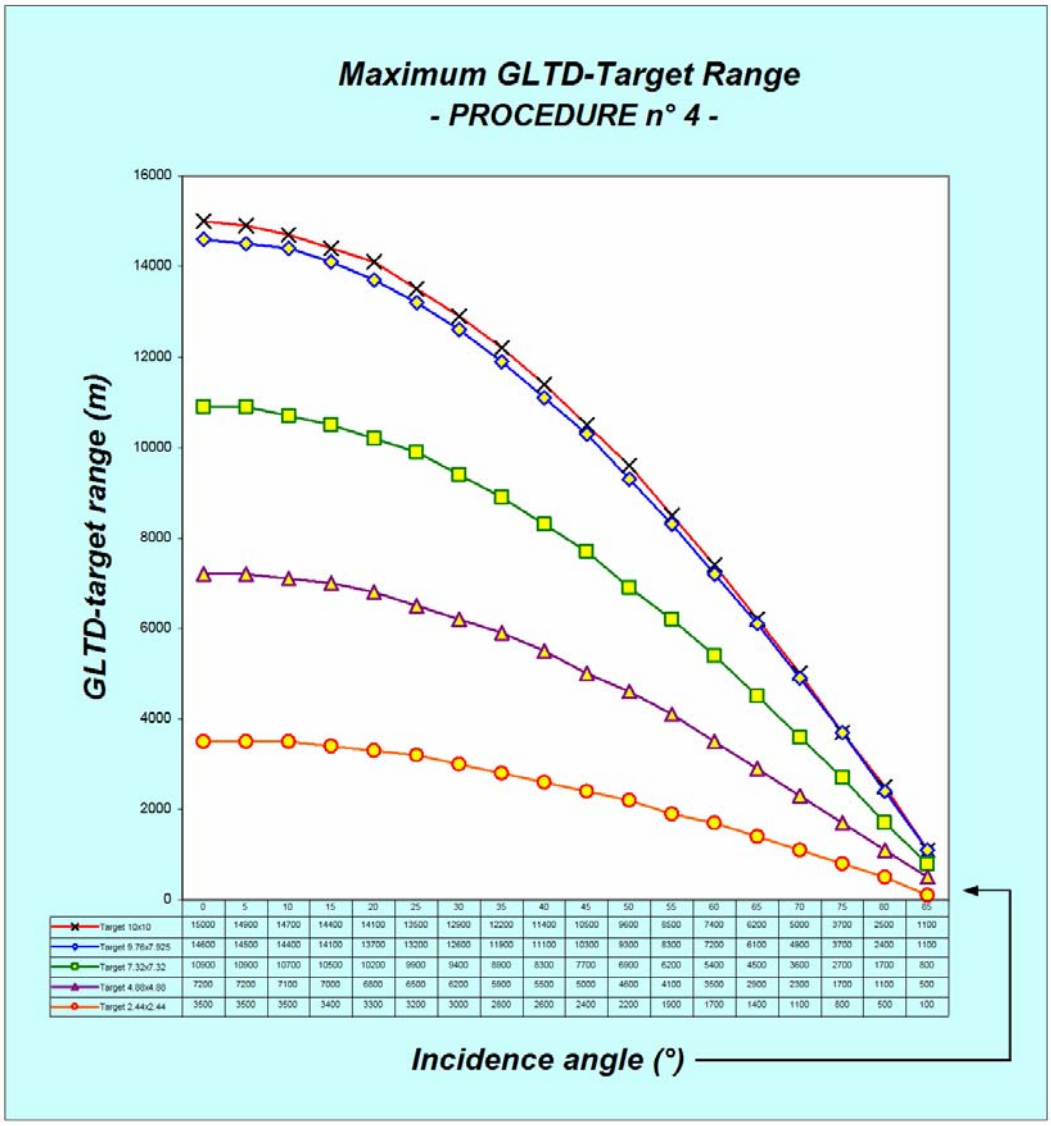

	0	5	10	15	20	25	30	35	40	45	50	55	60	65	70	75	80	85
Target 10x10	15000	14900	14700	14400	14100	13600	12900	12200	11400	10500	9600	8500	7400	6200	5000	3700	2500	1100
Target 9.76x7.925	14600	14500	14400	14100	13700	13200	12600	11900	11100	10300	9300	8300	7200	6100	4900	3700	2400	1100
Target 7.32x7.32	10900	10900	10700	10500	10200	9900	9400	8900	8300	7700	6900	6200	5400	4500	3600	2700	1700	800
Target 4.88x4.88	7200	7200	7100	7000	6800	6500	6200	5600	5500	5000	4600	4100	3500	2900	2300	1700	1100	500
Target 2.44x2.44	3500	3500	3500	3400	3300	3200	3000	2800	2600	2400	2200	1900	1700	1400	1100	800	500	100

Figure 10-5: Maximum ELOP-PLD Range vs. Incidence Angle (Procedure N° 4).

Together with slant-range restrictions, G-LTD safety Procedures N° 1 and N° 4 (described in Chapter 6) also include azimuth restrictions when the G-LTD is positioned at an elevated location with respect to the target. Taking into account both slant-range and azimuth restrictions (knowing the maximum altitude difference h_{max} between the target and the G-LTD locations), the G-EVP program computed the PILASTER areas where laser firing with the ELOP-PLD was permitted. These areas, identified as Safe Positioning Areas (SPA), calculated with the G-EVP program for both Procedure N° 1 and N° 4, are summarised in Figure 10-6 and in the Table 10-4 and Table 10-5.

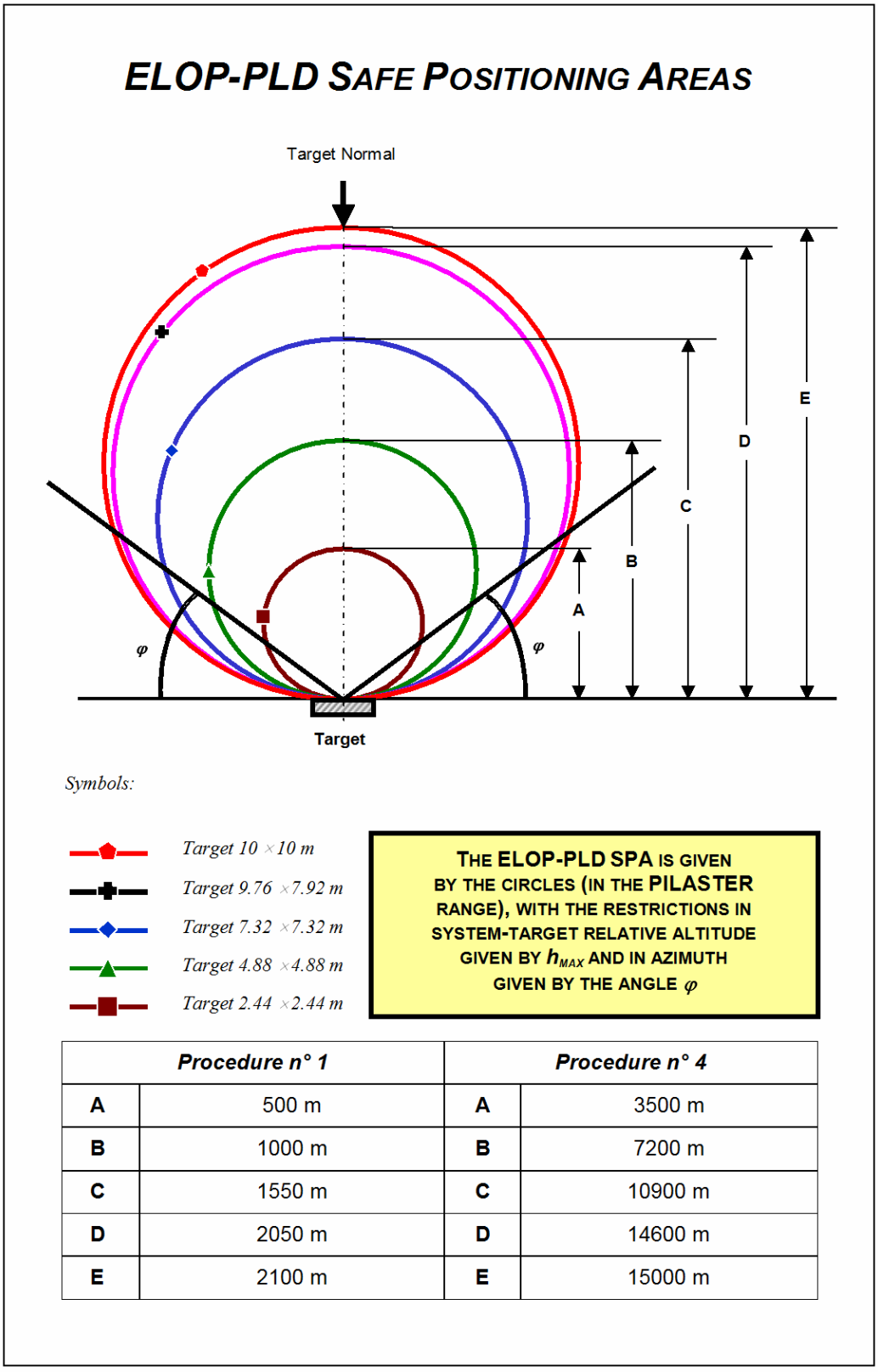

Procedure n° 1		Procedure n° 4	
A	500 m	A	3500 m
B	1000 m	B	7200 m
C	1550 m	C	10900 m
D	2050 m	D	14600 m
E	2100 m	E	15000 m

Figure 10-6: G-EVP Output – Safe Positioning Areas.

Table 10-4: G-EVP Output – Azimuth Limitations for Procedure N° 4

d (m)	h_{MAX} (m)	Procedure n° 4 - φ (°)				
		r_{MIN}=10 m	r_{MIN}=7.925 m	r_{MIN}=7.32 m	r_{MIN}=4.88 m	r_{MIN}=2.44 m
100	50	2	3	3	3	5
200	150	4	4	4	5	10
300	250	4	6	6	8	13
400	250	7	4	4	7	12
500	250	7	5	5	6	12
600	250	8	5	5	7	14
700	250	11	5	6	8	16
800	250	9	6	6	9	16
900	250	7	6	7	10	18
1000	250	8	7	7	10	19
1500	250	8	9	10	14	28
2000	250	10	12	13	18	37
2500	250	12	14	15	22	47
3000	250	13	17	18	27	60
3500	250	15	19	21	31	81
4000	250	17	22	23	36	n.a.
4500	250	19	24	26	40	n.a.
5000	250	21	27	29	45	n.a.
5500	250	23	29	32	51	n.a.
6000	250	25	32	35	58	n.a.
7000	250	30	38	42	76	n.a.
8000	250	34	44	49	n.a.	n.a.
9000	250	39	51	57	n.a.	n.a.
10000	250	43	59	68	n.a.	n.a.

n.a. = not available

Table 10-5: G-EVP Output – Azimuth Limitations for Procedure N° 1

d (m)	h_{MAX} (m)	Procedure n° 1 - φ (°)				
		r_{MIN}=10 m	r_{MIN}=7.925 m	r_{MIN}=7.32 m	r_{MIN}=4.88 m	r_{MIN}=2.44 m
100	50	5	5	6	9	16
200	150	10	11	13	19	38
300	250	13	15	17	24	51
400	250	15	19	20	31	79
500	250	17	20	23	33	n.a.
600	250	18	23	25	38	n.a.
700	250	21	26	28	45	n.a.
800	250	23	29	32	52	n.a.
900	250	26	33	36	60	n.a.
1000	250	28	37	40	71	n.a.
1500	250	43	59	68	n.a.	n.a.
2000	250	63	n.a.	n.a.	n.a.	n.a.

n.a. = not available

Some examples of ELOP-PLD safe positioning areas relative to the Procedures N° 1 and N° 4, plotted on the PILASTER ground range map area are shown in the Figure 10-7 through Figure 10-10.

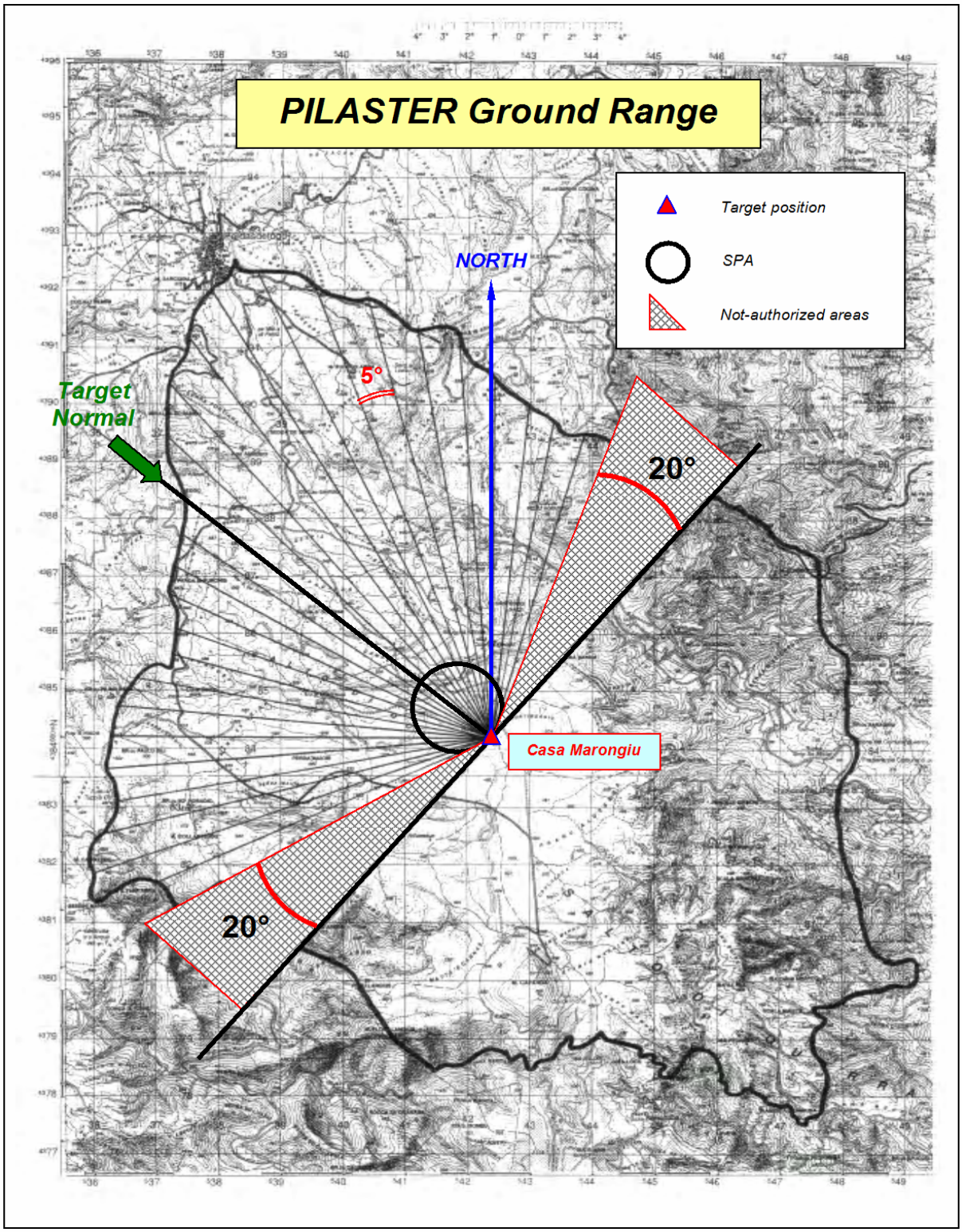

Figure 10-7: Procedure N° 1 – PILASTER SPA for r_{min} = 7.32 m, Maximum PLD-Target SR = 400 m and Maximum Relative Altitude Difference h_{max} = 250 m.

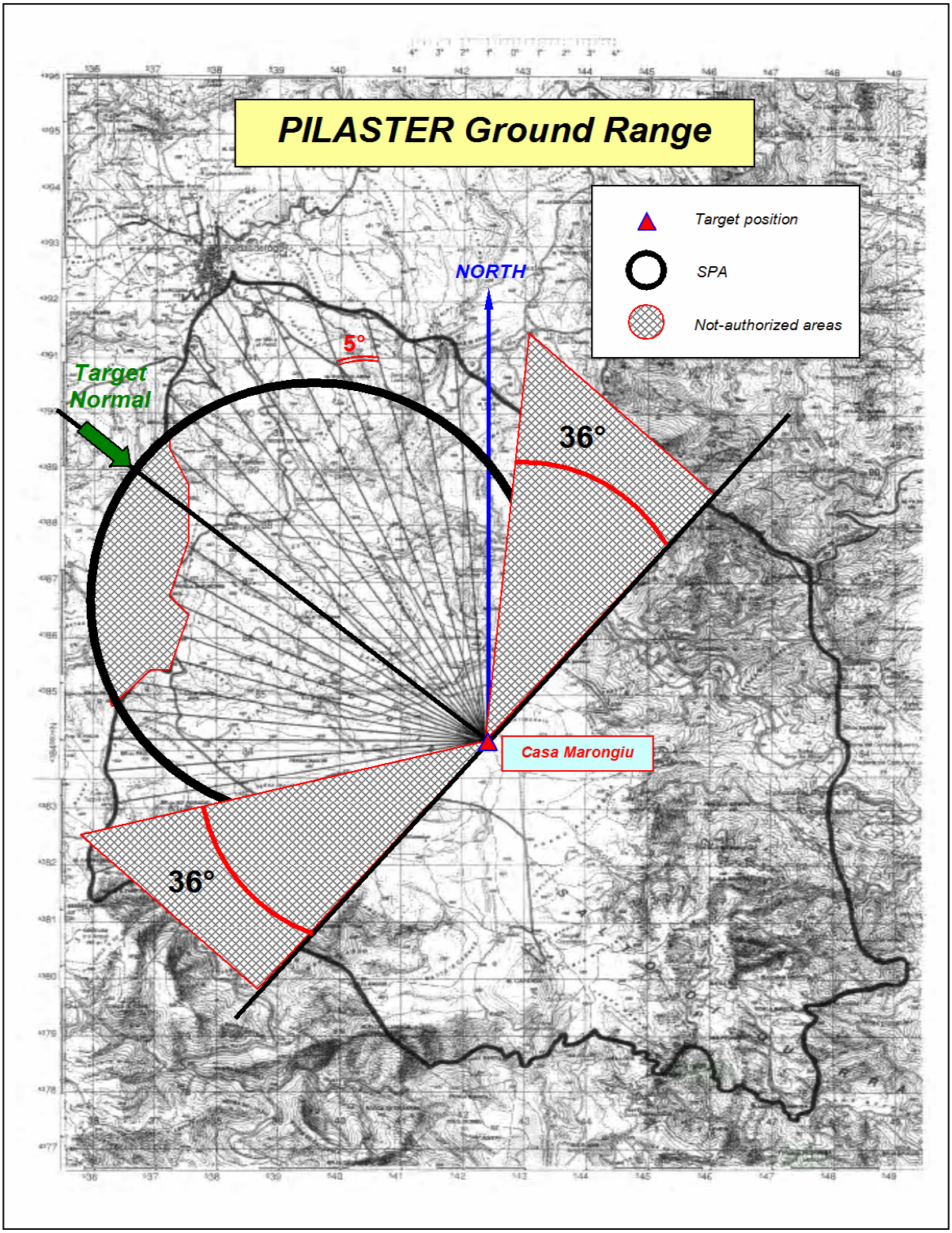

Figure 10-8: Procedure N° 4 – PILASTER SPA for r_{min} = 4.88 m, Maximum PLD-Target SR = 4 km and Maximum Relative Altitude Difference h_{max} = 250 m.

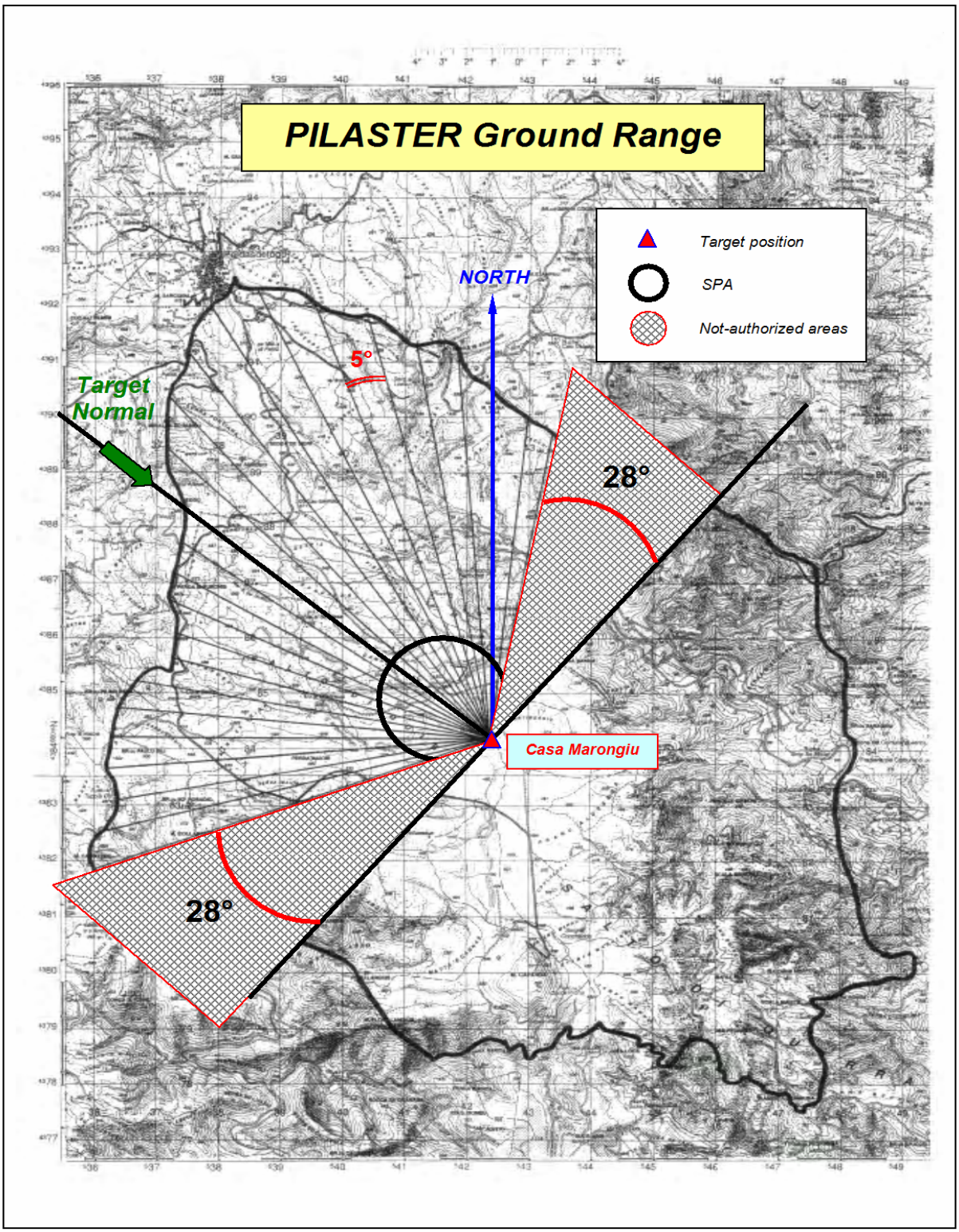

Figure 10-9: Procedure N° 1 – PILASTER SPA for r_{min} = 10 m, Maximum PLD-Target SR = 1 km and Maximum Relative Altitude Difference h_{max} = 250 m.

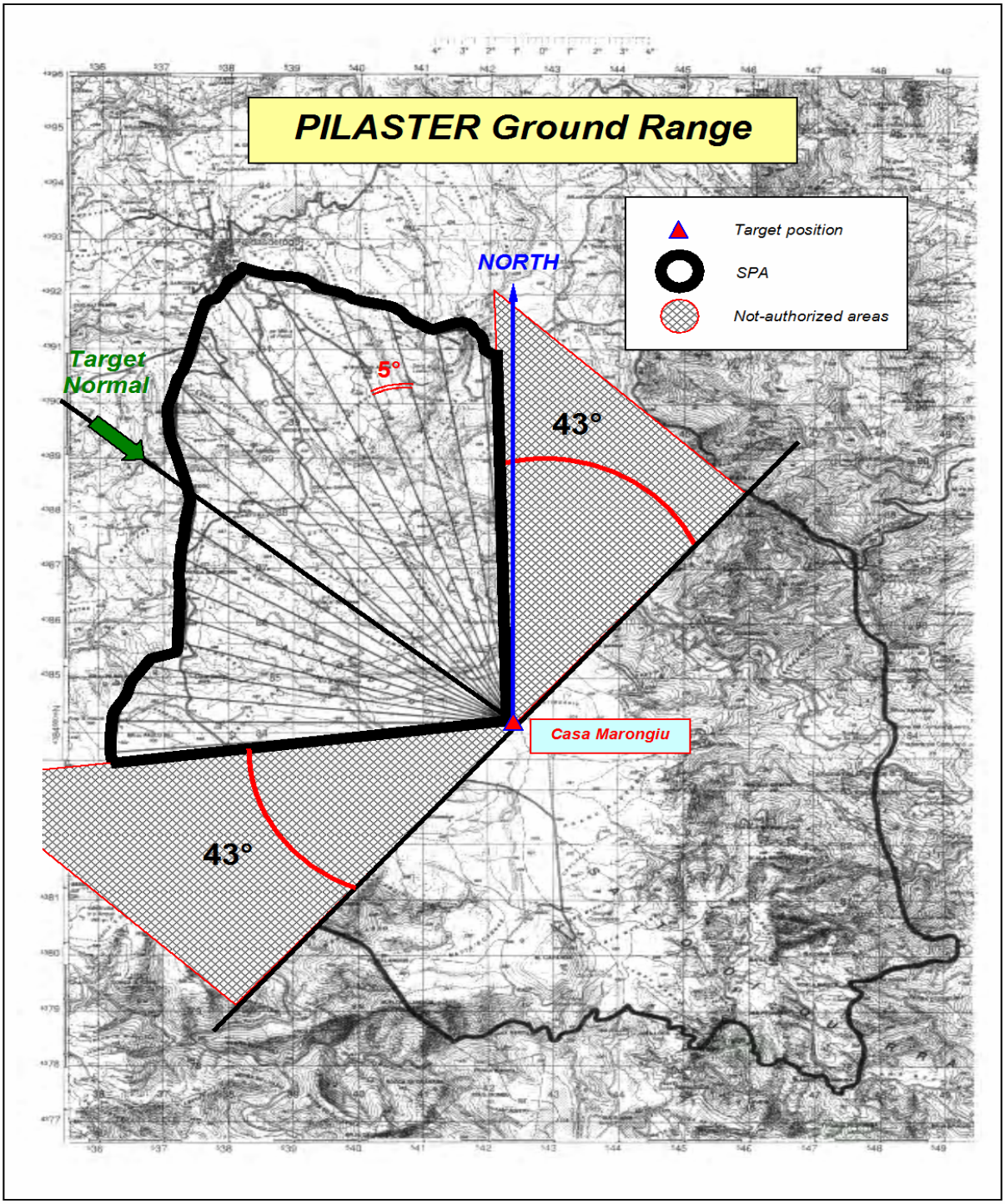

Figure 10-10: Procedure N° 4 – PILASTER SPA for r_{min} = 10 m, any PLD-Target SR in the Range Area and Maximum Relative Altitude Difference h_{max} = 250 m.

10.3 RANGE PERFORMANCE PREDICTION PROGRAM (RP3)

In the following paragraphs the Range Performance Prediction Program (RP3) is described. The RP3 program was implemented using the models described in Chapter 3, with the corrections to the ESLM

propagation model presented in the Chapters 8 and 9. Future versions of the program will be refined with further experimental results (LPDB).

10.3.1 RP3 Simulation Assumptions

The following general assumptions have been adopted for implementation of the RP3 program:

- **The Elder-Strong-Langer-Middleton (ESLM) model is used** to calculate the atmospheric attenuation coefficient. Corrections are adopted according to the results presented in Chapter 8 and 9.
- **The ESLM-LOWTRAN Model is used to calculate scattering due to rain**. Corrections are adopted according to the results presented in Chapter 9.
- **The output laser beam is assumed Gaussian**. A realistic assumption for most LTD currently in service.
- **Diffraction, jitter and spreading are not considered**, assuming an average irradiance at the target also having a Gaussian distribution.
- **The target reflecting surface is assumed planar and extended**: This assumption is acceptable considering the relative dimensions of the laser beam and most targets of practical interest.

Furthermore, either the **target directional reflectivity** (diffuse and specular reflection components) computed from BRDF data or the **diffuse reflectivity component** can be used for RP3 performance calculations.

10.3.2 RP3 Simulation Results

With the assumptions described above, we calculated the range performance of a particular LTD/LGB combination, using the data given in Table 10-6. These data are referred to generic LTD and LGB systems operating at a wavelength of 1.064 μm (not a real system).

Table 10-6: LTD/LGB Combination Characteristics

LTD	
Beam Diameter	60 mm
Beam Divergence	0.2 mrad
Wavelength	1.064 μm
Pick Energy	100 mJ
Pulse Duration	10^{-8} sec

LGB	
FOV	18°
MDPD	3 μW/m^2

Using the RP3 program, we evaluated the performance of this particular LTD/LGB combination in a certain operational scenario, with different atmospheric conditions. Furthermore, with the same atmospheric

conditions, we calculated the performance of the systems when used against target with different geometries (i.e., the maximum distance of the illuminating aircraft for an effective designation).

The curves shown in the Figure 10-11 through Figure 10-16 describe the range performance of the considered A-LTD/LGB combination, with different values of visibility (*V*) in the absence of rain. The RP3 input data included, together with parameters in Table 10-6, the relative humidity (*RH*) which was set to 100% at a temperature (*T*) of 30°C, and the target reflectivity which was assumed to be 10% (with a purely *Lambertian* distribution). In each graph, the range LTD-target is given as a function of the range LGB-target and a family of curves has been traced for different orientations of the target over the horizon (i.e., different values of the angles $Q_{t(MAX)}$ and $Q_{r(MAX)}$).

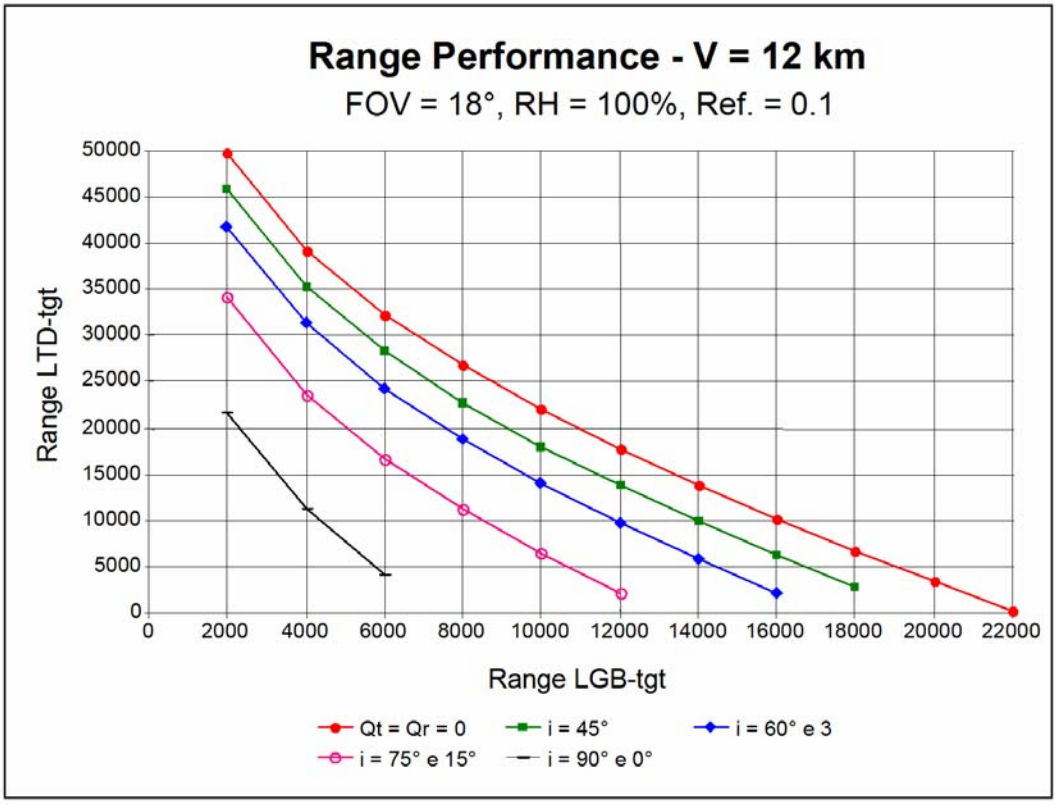

Figure 10-11: LTD/LGB Range Performance for V = 12 km.

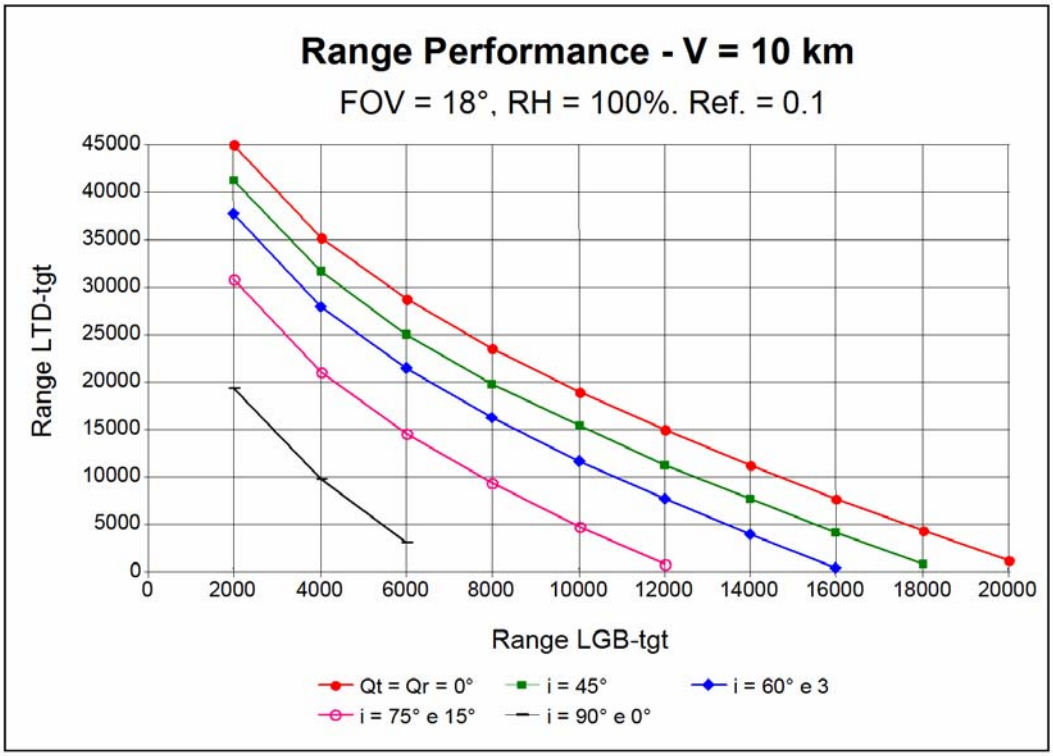

Figure 10-12: LTD/LGB Range Performance for V = 10 km.

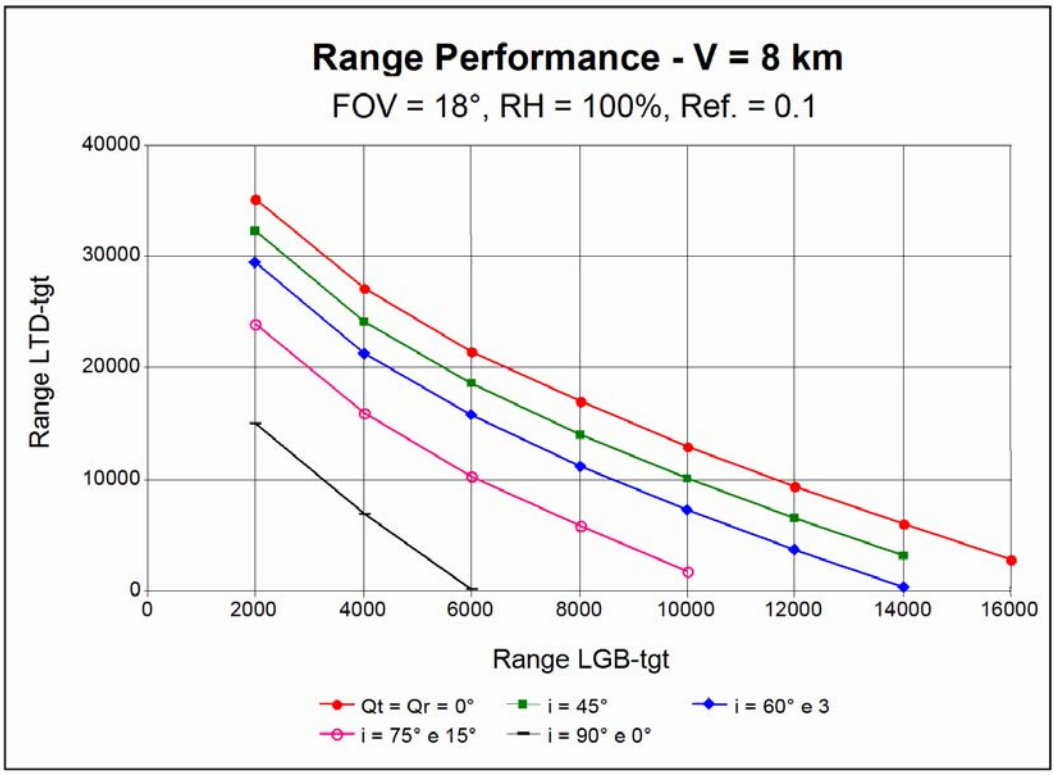

Figure 10-13: LTD/LGB Range Performance for V = 8 km.

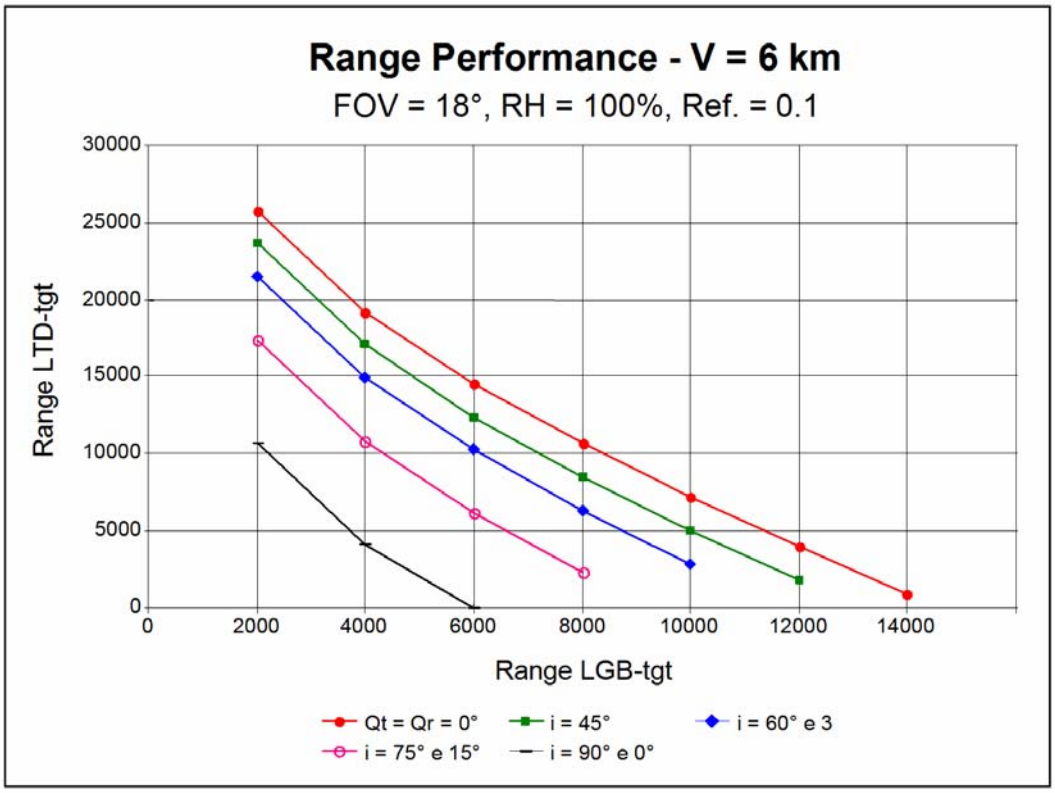

Figure 10-14: LTD/LGB Range Performance for V = 6 km.

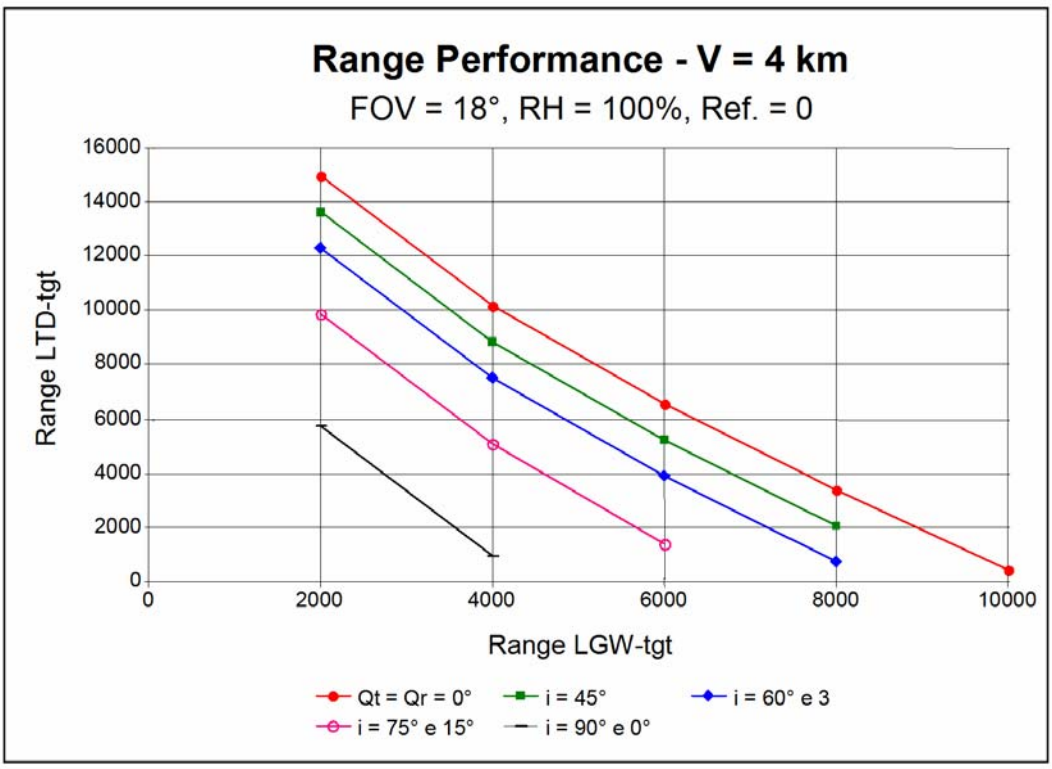

Figure 10-15: LTD/LGB Range Performance for V = 4 km.

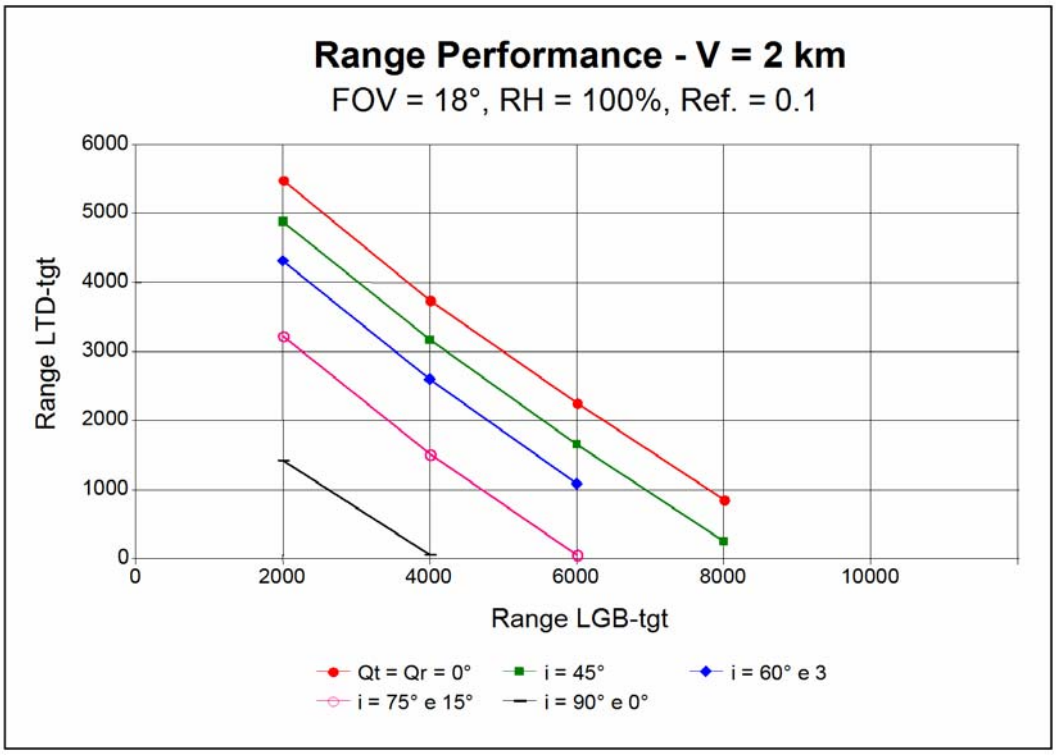

Figure 10-16: LTD/LGB Range Performance for V = 2 km.

Using the curves it is possible to determine whether or not the attack can be performed with a certain estimated minimum illumination time. Given the weapon initial conditions (i.e., velocity and trajectory) before designation is initiated, it is possible to estimate the designation time, taking into account the time required by the LGW from these initial conditions to stabilise towards the target (i.e., guided weapon ballistics). If the guidance algorithms are unknown it is possible to roughly estimate the designation time by assuming a straight trajectory of the bomb towards the target and a velocity in the final portion of its drop corresponding to the maximum theoretical velocity of the weapon. With these assumptions, the minimum theoretical range LGB-target before designation can be plotted in the graphs and consequently the maximum range of the aircraft at the beginning of the designation is determined. Obviously, when this range is less than the Target Lethal Range (TLR), the attack can not be performed successfully.

For instance, assuming a maximum LGB velocity of 800 ft/sec and a minimum designation time of 12 sec, the distance LGB-target before designation should not exceed 3 km, for an effective guidance. Plotting this value in Figure 10-17, we notice that in the worst geometric conditions the range LTD-target (illuminator-target) at the beginning of the designation is below the meteorological range (i.e., about 2 km for $V = 4$ km). For $V \geq 10$ km, laser illumination can be performed form a distance comparable to (or, theoretically, even grater than) the meteorological range.

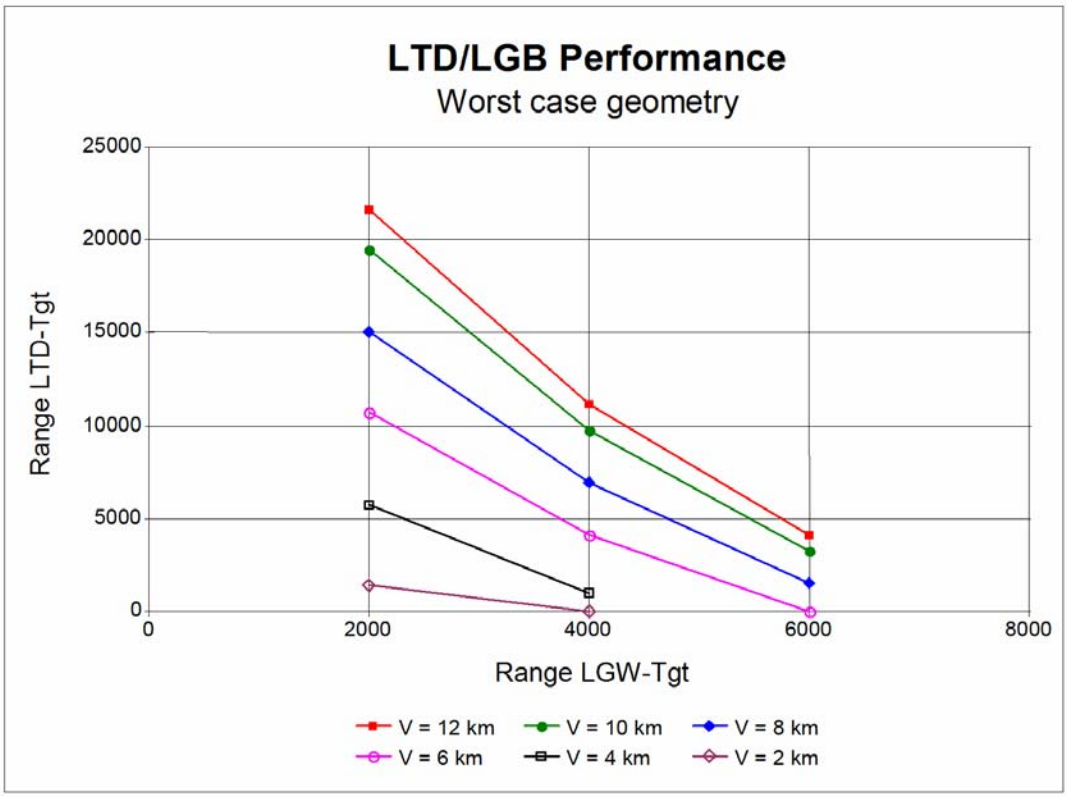

Figure 10-17: LTD/LGB Range Performance with Worst Case Geometry.

10.4 REMARKS

From the ALS/GLS eye-safety and performance analysis work described throughout this volume, and considering the results of the EVP and RP3 simulations performed, the following important conclusions were drawn:

- Both for ALS and for GLS systems, it is essential to define the maximum acceptable risk thresholds (i.e., maximum admitted probabilities of inadvertent hazardous events), before test/training missions can be performed at the ranges.
- ALS HOT attack missions are not allowed outside controlled test ranges (in which adequate personnel evacuation measures have been adopted).
- ALS Ferry Flights and DRY attack missions should be performed without electrical connection of the LDP laser system, in order to avoid any possible risk.
- For execution of Ferry Flights and DRY attach missions with an ALS system powered, it is essential to identify a (national) authority, either military or civilian, able to set the maximum acceptable risk thresholds.
- During test/training missions with ALS/GLS, cine-theodolites and other magnifying instruments can not be used at the ranges without adequate filtering.
- With typical A-LTD/LGB combinations, in dry-air conditions and visibility greater than 4 km, laser illumination can be performed successfully with the A-LTD carrying aircraft flying at a slant-range form the target not exceeding the meteorological range.

- With rain conditions, there is a considerable reduction of the range performance, limiting the operational use of most practical LTD/LGB combinations to the cases where the meteorological range is greater than 4 km.

10.5 ALS MISSION PLANNING PROGRAM (ALS-MPP)

As discussed in the previous chapters, prediction of laser systems performance requires appropriate knowledge of target signatures (e.g., reflectivity, BRDF/LCS), background characteristics, atmospheric attenuation, hardware performance (e.g., detectors, pointing/tracking and FOV), mission geometry (e.g., masking, laser grazing angle, aircraft and target motion) and, in some cases, human operator performance (e.g., target search and acquisition with TV/FLIR aids, manual laser firing). Furthermore, for mission planning purposes, it is also important to take into account eye-safety issues (especially for test and training activities with ALS systems). The kernel of a *Java* simulation program for a complete analysis of ALS systems performance and mission planning (test/training an operational missions), were developed during the PILASTER program. Particularly, the ALS-MPP kernel is composed of various classes, divided into three main groups: classes relative to the attack geometry and range performance model, classes relative to atmospheric laser beam propagation, and classes relative to the eye-safety analysis. The various classes were designed with the aim of developing a modular, flexible, and easy to modify kernel.

10.5.1 Future Developments

The ALS-MPP input and output interfaces have not been finalised jet, although a process in currently ongoing for developing the program interfaces in accordance with operational Flight Squadrons requirements. The current status of the ALS-MPP Input Interface (I/P-I) is illustrated in the Figure 10-18 through Figure 10-23. Currently, the I/P-I is composed by various data input panels and a global menu for managing the simulation. The first panel ('Meteo'), shown in Figure 10-18, allows to input the relevant weather parameters (i.e., rain type, absolute humidity and visibility).

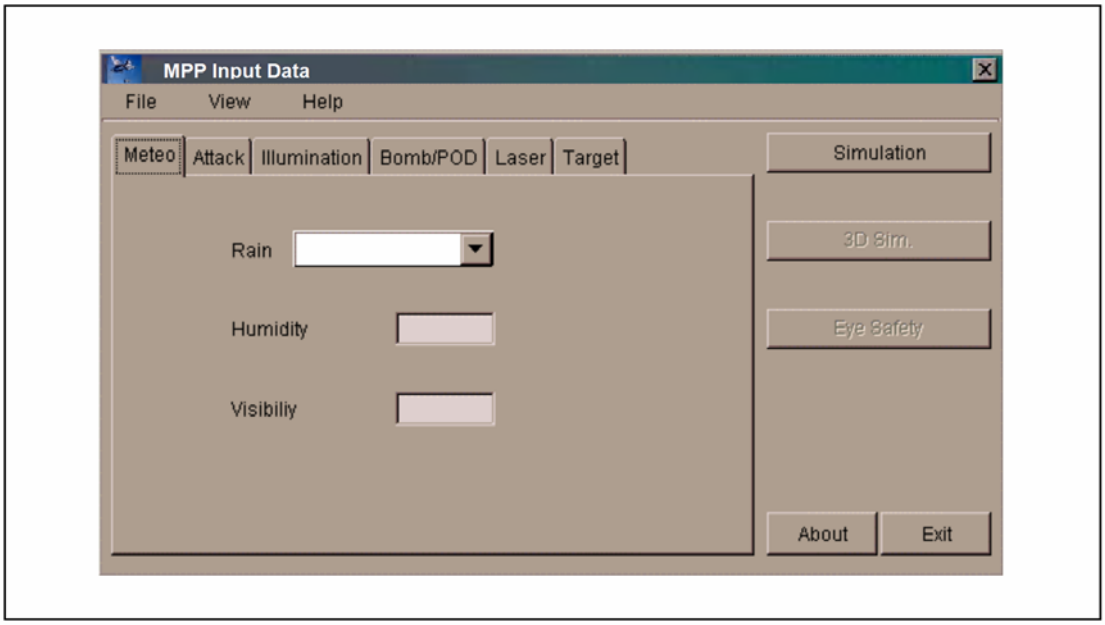

Figure 10-18: ALS-MPP I/P-I Panel 'Meteo'.

The second panel ('Attack') is relative to the attack parameters (Figure 10-19). The combined window (i.e., 'kind of attack') allows selection of 'dive', 'loft', or 'level' attack profiles. The sub-panels 'Altitude' and 'Preferred Directions' permit to input specific geometric constraints for the simulated mission.

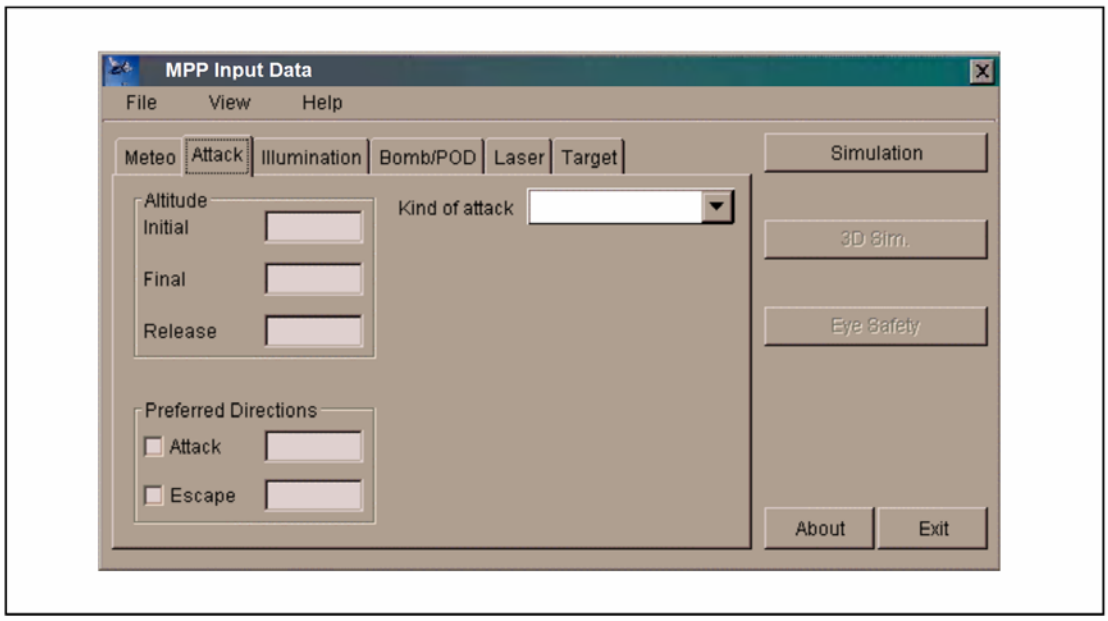

Figure 10-19: ALS-MPP I/P-I Panel 'Attack'.

The panel 'Illumination' includes selection of the type of attack (i.e., self-designation or co-operative) and, in case of a co-operative attack, the desired trajectory of the 'spiker' aircraft (Figure 10-20).

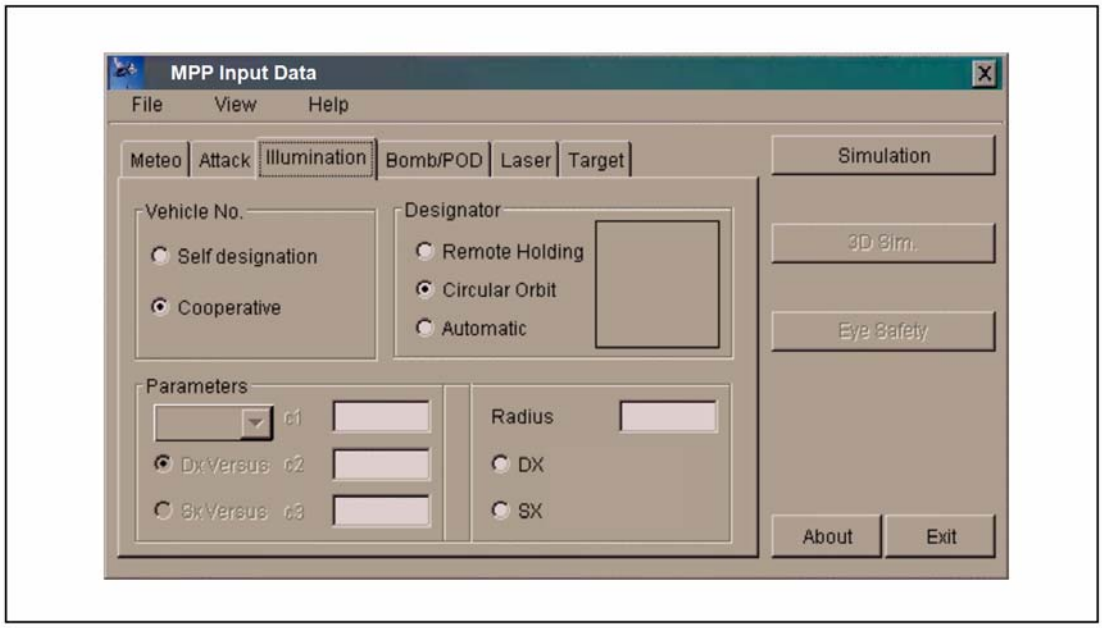

Figure 10-20: ALS-MPP I/P-I Panel 'Illumination'.

The fourth panel ('Bomb/POD') allows definition of the LGB and A-LTD aircraft configurations, with automatic selection (from a dedicated library) of the relative masking matrixes (Figure 10-21).

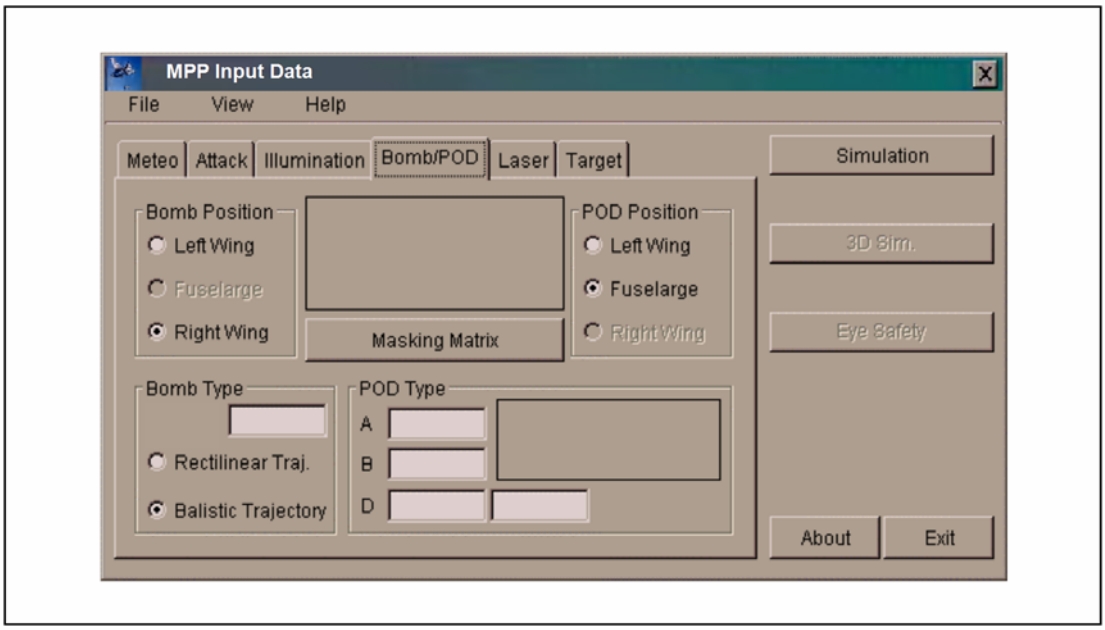

Figure 10-21: ALS-MPP I/P-I Panel 'Bomb/POD'.

The panel 'Laser' is available for input of the relevant A-LTD laser parameters (Figure 10-22).

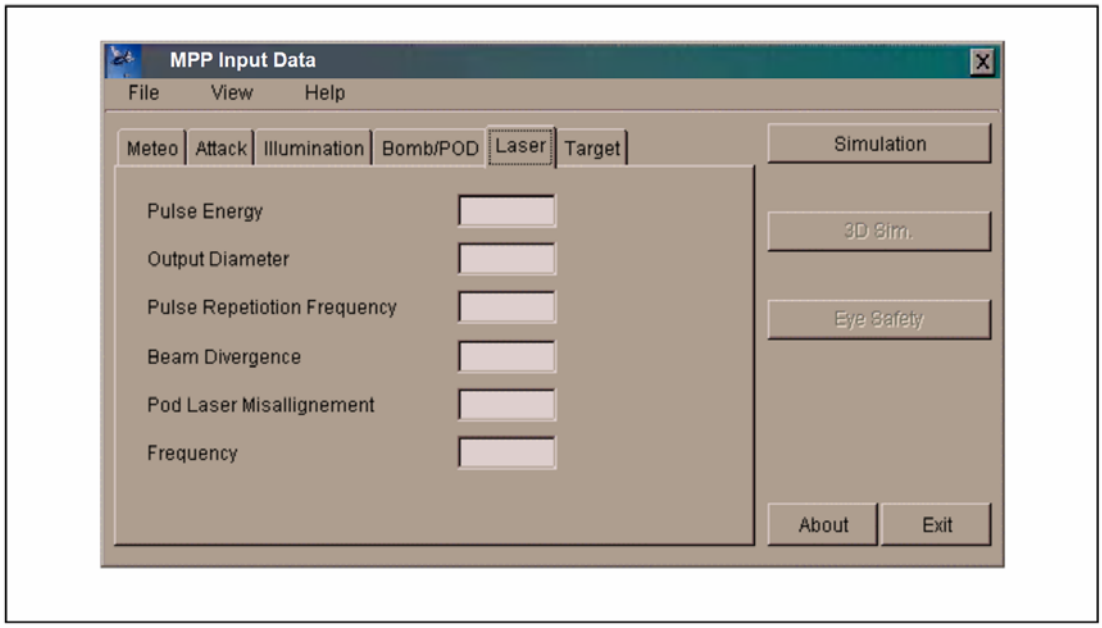

Figure 10-22: ALS-MPP I/P-I Panel 'Laser'.

The last panel is dedicated to the target description in terms of position, orientation, dimensions and material. A combined window is also available for selection of the type of co-ordinates to be used. In the

absence of accurate LCS or BRDF data, the program uses a library of diffuse reflectance data associated to the selectable target materials.

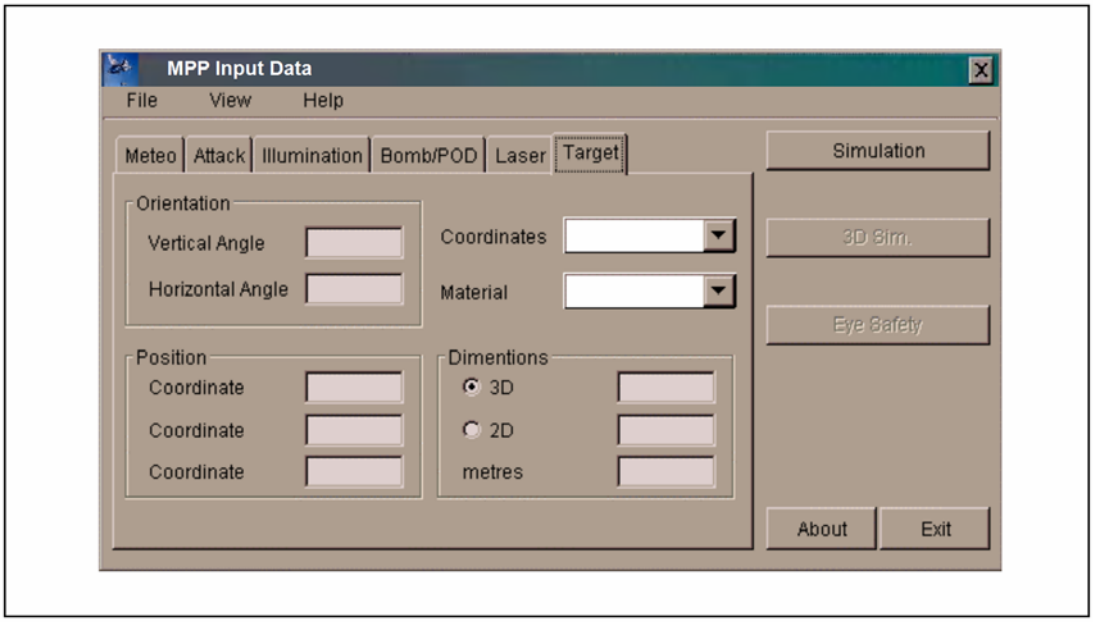

Figure 10-23: ALS-MPP I/P-I Panel 'Target'.

Examples of the current ALS-MPP Output Interfaces (O/P-I) are illustrated in Figure 10-24 through Figure 10-27.

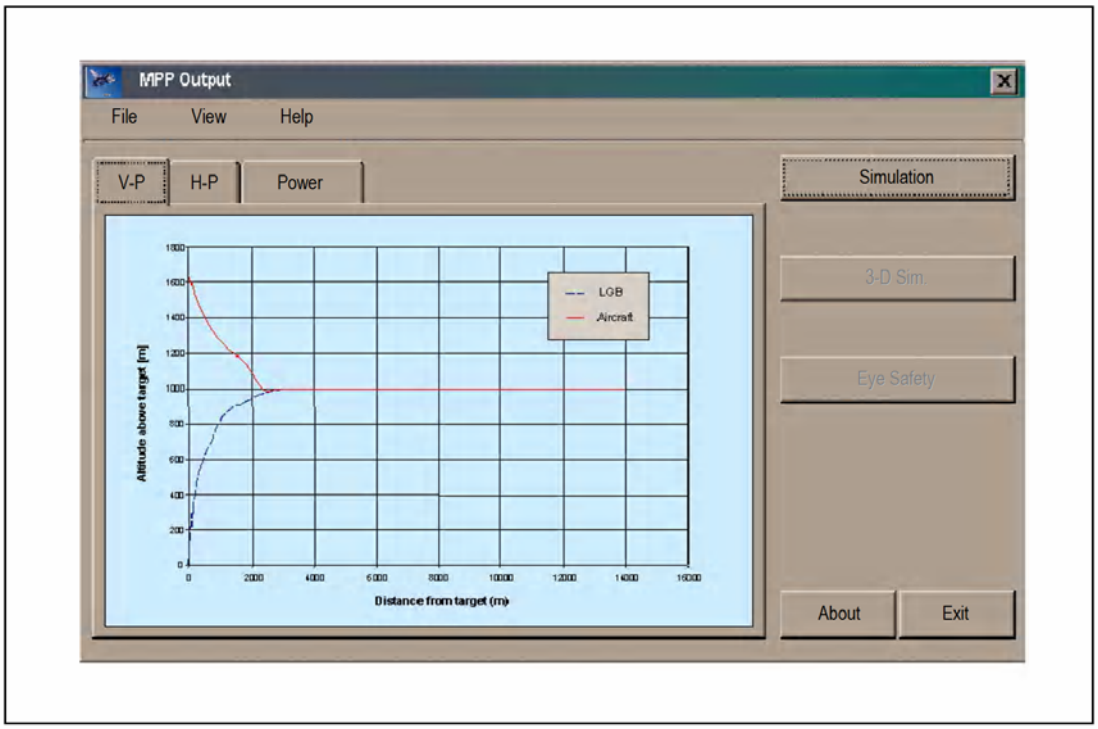

Figure 10-24: ALS-MPP Simulation O/P-I 'Vertical Profile' (V-P).

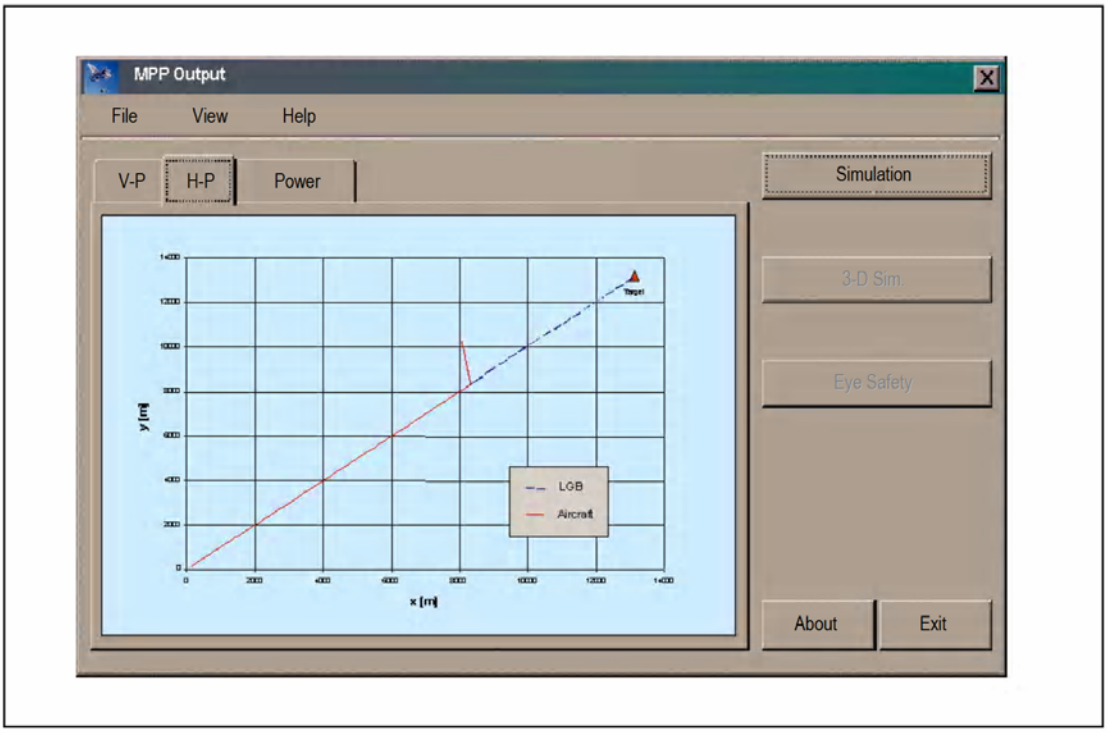

Figure 10-25: ALS-MPP Simulation O/P-I 'Horizontal Profile' (H-P).

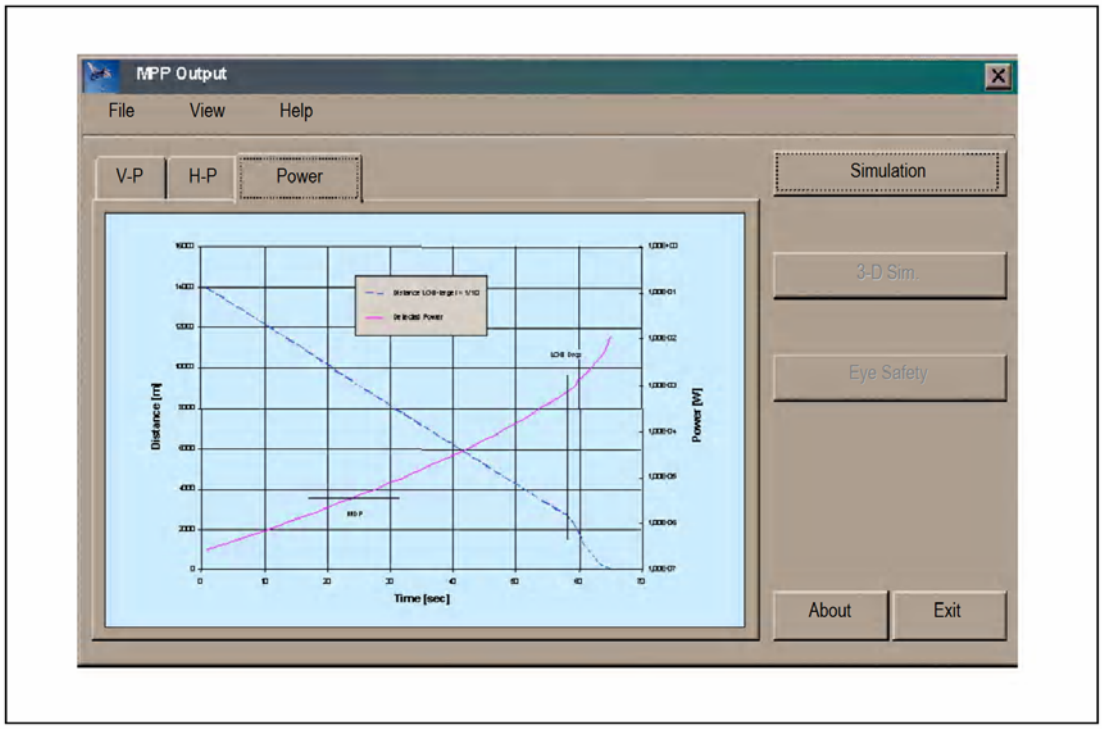

Figure 10-26: ALS-MPP O/P-I Simulation Panel 'Power'.

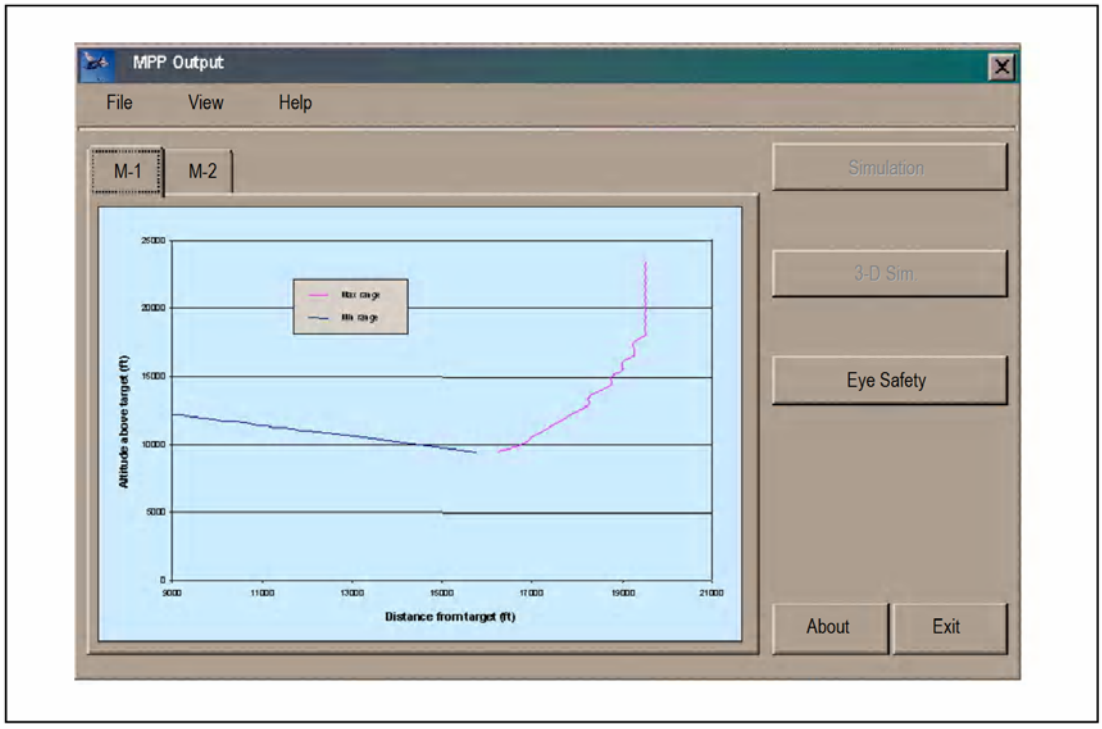

Figure 10-27: ALS-MPP Eye-Safety Analysis O/P-I for 'Mode-1' (M-1).

Figure 10-28 shows examples of the ALS-MPP 3-D visualisation tool.

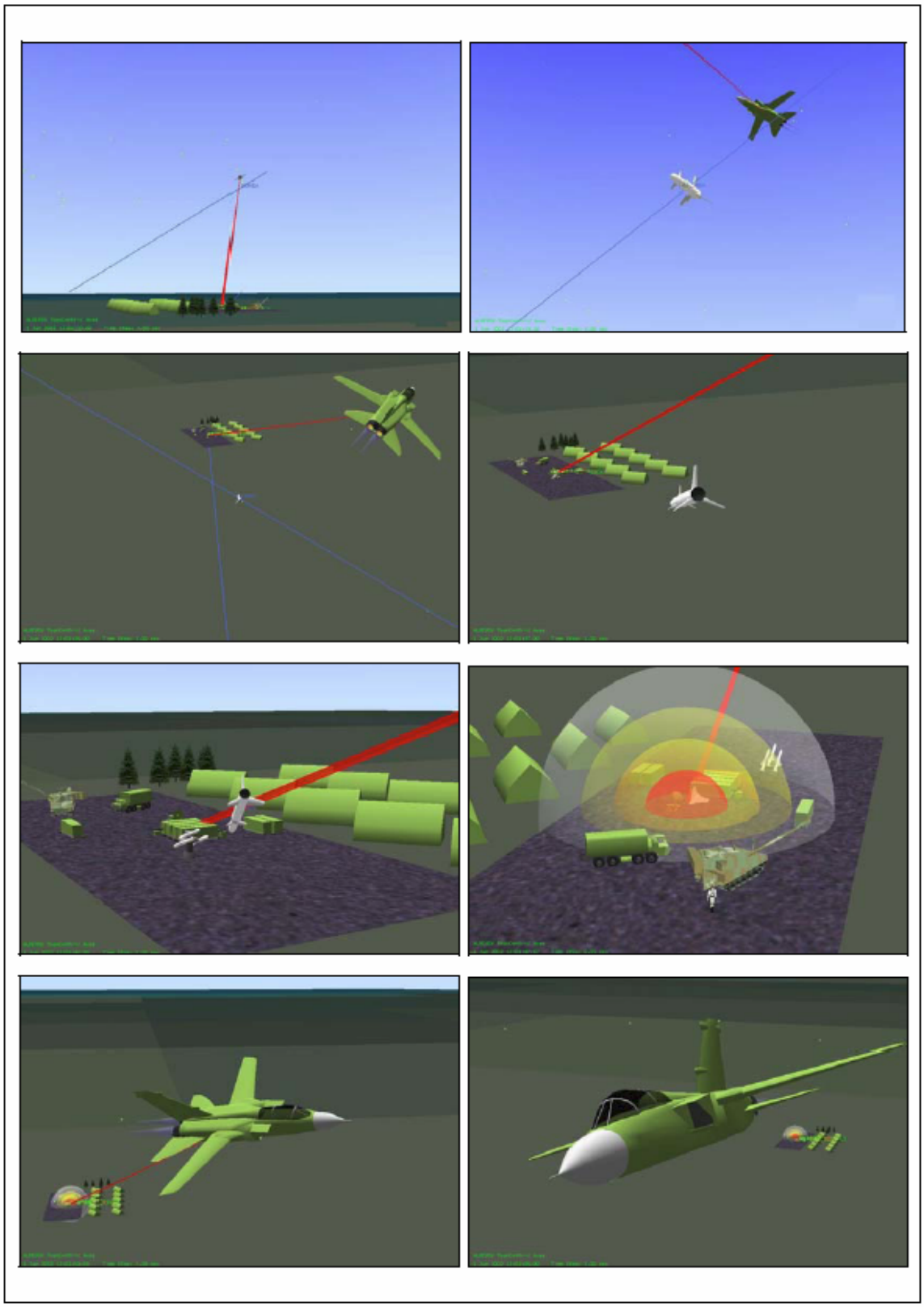

Figure 10-28: ALS-MPP 3-D Simulation O/P-I.